Title

Drumming motor sequence training induces apparent myelin remodelling in Huntington's disease: a longitudinal diffusion MRI and quantitative magnetization transfer study

Authors

Chiara Casella[1*], Jose Bourbon-Teles[1*], Sonya Bells[2], Elizabeth Coulthard[3], Greg D. Parker[1], Anne Rosser[4,6], Derek K. Jones[1,5], Claudia Metzler-Baddeley[1]

*These authors share first authorship

Affiliations

[1] Cardiff University Brain Research Imaging Centre (CUBRIC), School of Psychology, Cardiff University, Maindy Road, Cardiff, CF 24 4HQ, UK [2] The Hospital for Sick Children, Neurosciences and Mental Health, Toronto, M5G 1X8, Canada; [3] Clinical Neurosciences, University of Bristol, Bristol, BS10 5NB, UK, [4] School of Biosciences, Cardiff University, Museum Avenue, Cardiff, CF10 3AX, UK. [5] Mary MacKillop Institute for Health Research, Australian Catholic University, Melbourne, Victoria 3065, Australia.[6] Department of Neurology and Psychological Medicine, Hayden Ellis Building, Maindy Rd, CF24 4HQ

Running title

Training-associated myelin-remodelling in HD.

Corresponding author

Chiara Casella, CUBRIC, Maindy Road, Cardiff CF24 4 HQ, CasellaC@cardiff.ac.uk.

1. Abstract

Background: Impaired myelination may contribute to Huntington's disease (HD) pathogenesis. **Objective:** This study assessed differences in white matter (WM) microstructure between HD patients and controls, and tested whether drumming training stimulates WM remodelling in HD. Furthermore, it examined whether training-induced microstructural changes are related to improvements in motor and cognitive function. **Methods:** Participants undertook two months of drumming exercises. Working memory and executive function were assessed before and post-training. Changes in WM microstructure were investigated with diffusion tensor magnetic resonance imaging (DT-MRI)-based metrics, the restricted diffusion signal fraction (Fr) from the composite hindered and restricted model of diffusion (CHARMED) and the macromolecular proton fraction (MPF) from quantitative magnetization transfer (qMT) imaging. WM pathways linking putamen and supplementary motor areas (SMA-Putamen), and three segments of the corpus callosum (CCI, CCII, CCIII) were studied using deterministic tractography. Baseline MPF differences between patients and controls were assessed with tract-based spatial statistics (TBSS). **Results:** MPF was reduced in the mid-section of the CC in HD subjects at baseline, while a significantly greater change in MPF was detected in HD patients relative to controls in the CCII, CCIII, and the right SMA-putamen post-training. Further, although patients improved their drumming and executive function performance**,** such improvements did not correlate with microstructural changes. Increased MPF suggests training-induced myelin changes in HD. **Conclusions:** Though only preliminary and based on a small sample size, these results suggest that tailored behavioural stimulation may lead to neural benefits in early HD, that could be exploited for delaying disease progression.

Key words

Huntington's disease, drumming training, white matter, myelin, diffusion MRI

2. Introduction

2.1 The Pathology of Huntington's disease

Huntington's disease (HD) is a genetic, neurodegenerative disorder caused by an expansion of the CAG repeat within the *huntingtin* gene, leading to debilitating cognitive, psychiatric, and motor symptoms. In addition to striatal grey matter (GM) degeneration [1], HD pathology has been linked to white matter (WM) changes [2–9]. Additionally, an increasing body of research suggests that myelin-associated biological processes at the cellular and molecular level contribute to WM abnormalities [10–15]. Myelin is a multi-layered membrane sheath wrapping axons and is produced by oligodendrocytes. Axon myelination is vital during brain development and critical for healthy brain function [16]. Oligodendrocyte/myelin dysfunction can slow down or stop otherwise fast axonal transport, which in turn can result in synaptic loss and eventually axonal degeneration [17].

2.2 Interventions and Brain Plasticity

As HD is caused by a single-gene, it is an ideal model to study neurodegeneration as a whole, and test for possible beneficial interventions that can slow or suppress disease onset. Despite this, no disease-modifying treatment is approved for patients with HD at present. Recent developments in gene therapy have generated much excitement. However, these have yet to be proved to lead to measurable changes in disease progression [18]. Furthermore, a number of questions linger, for example on the relative strength of different approaches and the possible

side effects of each therapy [19]. Importantly, these treatments aim to modify and not cure the disease, and while symptomatic therapies for HD are present, and are used for treating chorea and some of the psychiatric symptoms, their effectiveness varies between patients and may lead to clinically significant side-effects [18]. This stresses the need to develop better symptomatic therapies to aid patients and manage HD symptoms.

Environmental stimulation and behavioural interventions may have the potential to reduce disease progression and delay disease onset [20–22]. Furthermore, previous studies have detected training-related changes in the WM of both healthy controls [23,24] and patients, including subjects with HD [25]. For example, DT MRI studies have shown microstructural WM changes following balance training in healthy [24] and traumatic brain injury young adults [26]. Other imaging studies have shown DT MRI changes as a result of juggling [27], abacus training [28], extensive piano practice [29,30], working memory training [31], reasoning training [32], and meditation training [33].

Converging evidence implicates myelin plasticity as one of the routes by which experience shapes brain structure and function [27,34–38]. Plastic changes in myelination may be implicated in early adaptation and longer-term consolidation and improvement in motor tasks [39–42]. Changes in myelin-producing oligodendrocytes and in GM and WM microstructure have been reported within the first hours of skill acquisition [43,44], implying that experience can be quickly translated into adaptive changes in the brain.

This study assessed whether two months of drumming training, involving practising drumming patterns in ascending order of difficulty, could trigger WM microstructural changes, and potentially myelin remodelling, in individuals with HD.

Specifically, we hypothesised that changes in *microstructural* metrics would be more marked in patients than in healthy subjects, based on reports of larger training-associated changes in structural MRI metrics in patient populations than in healthy controls [34].

The drumming intervention was designed to target cognitive and motor functions known to be mediated by cortico-basal ganglia loops. More specifically the training focused on the learning of novel motor sequences and their rhythm and timing, engaging executive processes known to be impaired in HD [45]. These included focused attention (e.g. paying attention to the drumming sequence), multi-tasking attention (e.g. listening and movement execution), movement-switching (e.g. switching between dominant and non-dominant hand) and response speed [25]. At the anatomical level, attention and executive functions rely on cortico-basal ganglia loops involving the striatum, which also plays a fundamental role in motor control and motor learning [46,47]. This shared reliance on overlapping cortico-basal ganglia networks may contribute to the beneficial effects of physical exercise on executive functioning in healthy older adults [48], and in patients with Parkinson's disease [49]. Additionally, in a previous pilot study assessing the feasibility of the present drumming training, we observed WM changes and improvements in executive functions in HD patients following the intervention [25].

Previous WM plasticity neuroimaging studies [27,50] have predominantly employed indices from diffusion tensor MRI (DT-MRI) [51]. However, while sensitive, such measures are not specific to changes in specific sub-compartments of WM microstructure, challenging the interpretation of any observed change in DT-MRI indices [52,53]. To improve compartmental specificity beyond DT-MRI, the present study explored changes in the macromolecular proton fraction (MPF) from quantitative

magnetization transfer (qMT) [54] imaging and the restricted diffusion signal fraction (Fr) from the composite hindered and restricted model of diffusion (CHARMED) [55]. Fractional anisotropy (FA) and radial diffusivity (RD) from DT-MRI [51] were included for comparability with previous training studies [27,56,57].

The MPF has been proposed as a proxy MRI marker of myelin [58]. Accordingly, histology studies show that this measure reflects demyelination accurately in Shiverer mice [59], is sensitive to de-myelination in multiple sclerosis patients [60] and reflects WM myelin content in post-mortem studies of multiple sclerosis brains [61]. Fr, on the other hand, represents the fraction of signal-attenuation that can be attributed to restricted diffusion, which is presumed to be predominantly intra-axonal, and therefore provides a proxy measure of axonal density [62].

Training effects were investigated in WM pathways linking the putamen and the supplementary motor area (SMA-Putamen), and within three segments of the corpus callosum (CCI, CCII, CCIII). The SMA has efferent and afferent projections to the primary motor cortex and is involved in movement execution, and previous work has reported altered DT-MRI metrics in the putamen-motor tracts of symptomatic HD patients [63]. The anterior and anterior-mid sections of the corpus callosum contain fibres connecting the motor, premotor and supplementary motor areas in each hemisphere [64]. Previous work has demonstrated a thinning of the corpus callosum in post-mortem HD brains [65], altered callosal DT-MRI metrics in both pre-symptomatic and symptomatic HD patients [66,67], and a correlation between these metrics and performance on motor function tests [68]. Given previous reports of an effect of motor learning on myelin plasticity [38], we expected changes following training to be more marked in MPF, as compared to the other non-myelin sensitive

metrics assessed in this study. We also investigated the relationship between training-associated changes in MRI measures, and changes in drumming performance and cognitive/executive function. Finally, as previous evidence has shown widespread reductions in MPF in premanifest and manifest HD patients [69], we used tract-based spatial statistics (TBSS) [70] to investigate patient-control differences in MPF before training, across the whole brain; this aided the interpretation of the post-training microstructure changes we detected.

3. Materials and Methods

3.1 Participants

The study was approved by the local National Health Service (NHS) Research Ethics Committee (Wales REC 1 13/WA/0326) and all participants provided written informed consent. All subjects were drumming novices and none had taken part in our previously-reported pilot study [25]. Fifteen HD patients were recruited from HD clinics in Cardiff and Bristol. Genetic testing confirmed the presence of the mutant huntingtin allele. Thirteen age, sex, and education-matched healthy controls were recruited from the School of Psychology community panel at Cardiff University and from patients' spouses, carers or family members. The inclusion criteria were the following: no history of head injury, stroke, cerebral haemorrhages or any other neurological condition; eligible for MRI scanning; stable medication for at least four weeks prior to the study.

Of the recruited sample, two patients were not MRI compatible, four withdrew during the study and one patient's MRI data had to be excluded due to excessive motion. Therefore, while drumming performance and cognitive data from 11 patients were assessed, only 8 patients had a complete MRI dataset. One control participant

was excluded due to an incidental MRI finding, two participants dropped out of the study and a fourth participant was not eligible for MRI. In total, we assessed drumming and cognitive tests performance in 8 controls, while MRI data from nine controls were available for analyses. Table 1 summarizes patients demographic and background clinical characteristics. Most patients were at early disease stages, however two were more advanced, as shown by their Total Motor Score (TMS; 69 and 40, respectively) and Functional Assessment Score (FAS; 18 and 17, respectively). Table 2 summarizes demographic variables and performance in the Montreal Cognitive Assessment (MoCA) [71] and in the revised National Adult Reading Test (NART-R) (Nelson, 1991) for patients and controls. While the groups did not differ significantly in age, controls were on average slightly older, performed significantly better on the MoCA, and had a significantly higher NART-IQ than patients.

3.2 Training intervention: Drumming-based rhythm exercises

The rhythm exercise and drumming training previously described in [25] was applied. Participants were provided with twenty-two 15 min training sessions on CDs, a pair of Bongo drums and a drumming diary and could practise at home. They were asked to exercise for 15 min per day, 5 times per week, for 2 months and to record the date and time of each exercise in their diary. Each training session introduced a drumming pattern based on one of the following rhythms: Brazilian samba, Spanish rumba, West-African kuku and Cuban son. After a brief warm up, trainees were encouraged to drum along with the instructor, initially with each hand separately and then with both hands alternating, starting with the dominant hand first and then reversing the order of the hands. The first exercises were based on very simple, slow,

and regular patterns but the level of complexity and speed increased over the training sessions.

Importantly, each individual progressed through the training adaptively at their own pace i.e., as long as they exercised for the specified time, they could repeat each session as often as they felt necessary to master it. To maintain engagement and motivation, the training incorporated pieces of music based on rhythms participants had learned and could drum along to. The researcher (JBT) supervised the first training sessions and then remained in regular telephone contact (at least once a week) with each participant throughout the intervention. Whenever possible, carers and/or spouses were involved in the study to support the training. Control participants started with Session 3 since the first two exercises were built on a very low level of complexity, with slow, regular patterns of movement required. Patients, on the other hand, started with simpler exercises, but could progress to the following sessions whenever they felt comfortable.

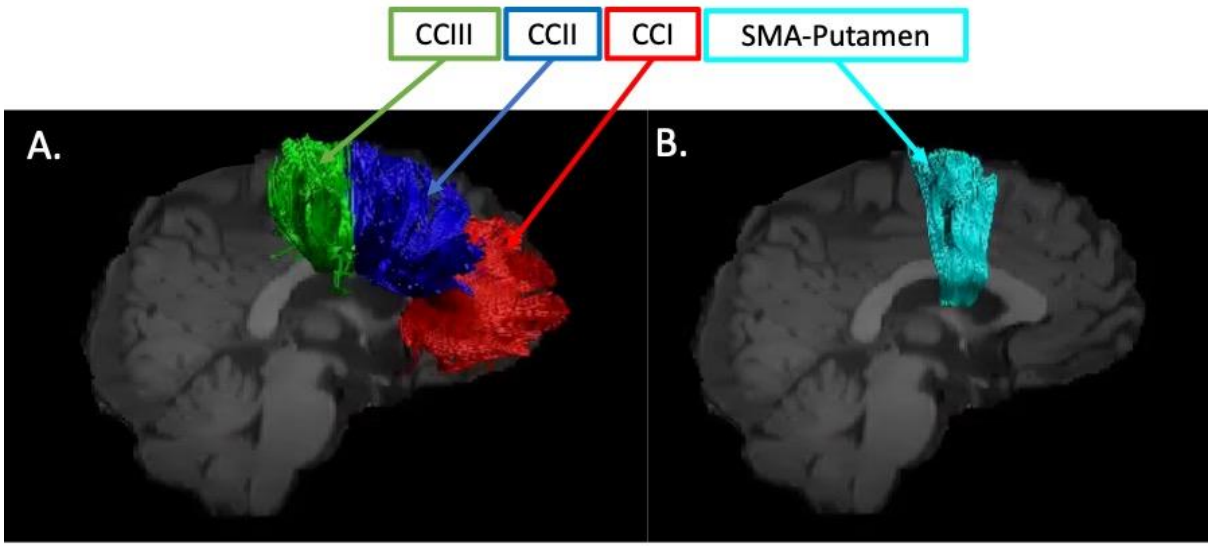

Figure 1.

3.3 Drumming assessment

Progress in drumming ability was assessed by digitally recording participants' drumming performance for three patterns of ascending levels of difficulty (easy, medium and hard), which were not part of the training sessions, at baseline and after the training. Each recording was judged by an independent rater, blind to group and time, according to an adopted version of the Trinity College London marking criteria for percussion (2016) (www.trinitycollege.com).

3.4 Cognitive assessments

Different aspects of cognition and executive function were assessed before and after the training as previously described [25]. Multi-tasking was assessed with a dual task requiring simultaneous box crossing and digit sequences repetition [73]. Attention switching was assessed with the trails test (VT) requiring the verbal generation of letter and digit sequences in alternate order relative to a baseline condition of generating letter or digit sequences only (69). Distractor suppression was tested with the Stroop task involving the naming of incongruent ink colours of colour words. Verbal and category fluency were tested using the letter cues "F", "A", "S" and "M", "C", "R" as well as the categories of "animals" and "boys' names" and "supermarket items" and "girls' names" respectively [74]. In total, we assessed 7 outcome variables, and percentage change scores in performance were computed for each of these variables (Table 3).

3.5 MRI data acquisition

MRI data were acquired on a 3 Tesla General Electric HDx MRI system (GE Medical Systems, Milwaukee) using an eight channel receive-only head RF coil at the Cardiff University Brain Research Imaging Centre (CUBRIC). The MRI protocol comprised the following images sequences: a high-resolution fast spoiled gradient echo (FSPGR) T_1-weighted (T_1-w) sequence for registration; a diffusion-weighted spin-echo echo-planar sequence (SE\EPI) with 60 uniformly distributed directions ($b = 1200$ s/mm^2), according to an optimized gradient vector scheme [75]; a CHARMED acquisition with 45 gradient orientations distributed on 8 shells (maximum b-value = 8700s/mm^2) [55]; and a 3D MT-weighted fast spoiled gradient recalled-echo (FSPGR) sequence [76]. The acquisition parameters of all scan sequences are reported in Table 4. Diffusion data acquisition was peripherally gated to the cardiac cycle. The off-resonance irradiation frequencies (Θ) and their corresponding saturation pulse amplitude (ΔSAT) for the 11 Magnetization transfer (MT) weighted images were optimized using Cramer-Rao lower bound optimization [76].

3.6 MRI data processing

The diffusion-weighted data were corrected for distortions induced by the diffusion-weighted gradients, artefacts due to head motion and EPI-induced geometrical distortions by registering each image volume to the T_1-w anatomical images [77], with appropriate reorientation of the encoding vectors [78], all done in ExploreDTI (Version 4.8.3) [79]. A two-compartment model was fitted to derive maps of FA and RD in each voxel [80]. CHARMED data were corrected for motion and distortion artefacts according to the extrapolation method of [81] The number of distinct fiber populations (1, 2, or 3) in each voxel was obtained using a model selection approach [52], and Fr was calculated per voxel with an in-house software [52] coded

in MATLAB (The MathWorks, Natick, MA). MT-weighted SPGR volumes for each participant were co-registered to the MT-volume with the most contrast using an affine (12 degrees of freedom, mutual information) registration to correct for inter-scan motion using Elastix [82]. The 11 MT-weighted SPGR images and T_1 map were modelled by the two pool Ramani's pulsed MT approximation [83,84], which included corrections for amplitude of B_0 field inhomogeneities. This approximation provided MPF maps, which were nonlinearly warped to the T_1-w images using the MT-volume with the most contrast as a reference using Elastix (normalized mutual information cost function) [82].

3.7 Deterministic Tractography

Training-related changes in FA, RD, Fr, and MPF were quantified using a tractography approach in pathways interconnecting the putamen and the supplementary motor area bilaterally (SMA-Putamen), and within three segments of the corpus callosum (CCI, CCII and CCIII) [64] (Figure 1).

Whole brain tractography was performed for each participant in their native space using the damped Richardson-Lucy algorithm [85], which allows the recovery of multiple fiber orientations within each voxel including those affected by partial volume. The tracking algorithm estimated peaks in the fiber orientation density function (fODF) by selecting seed points at the vertices of a 2×2×2 mm grid superimposed over the image and propagated in 0.5-mm steps along these axes re-estimating the fODF peaks at each new location [86]. Tracks were terminated if the fODF threshold fell below 0.05 or the direction of pathways changed through an angle greater than 45° between successive 0.5 mm steps. This procedure was then repeated by tracking in the opposite direction from the initial seed-points.

The WM tracts of interest were extracted from the whole-brain tractograms by applying way-point regions of interest (ROI) [87]. These were drawn manually by one operator (JBT) blind to the identity of each dataset on color-coded fiber orientation maps in native space guided by the following anatomical landmark protocols (Figure 2).

3.7.1 Corpus callosum

Reconstruction of the CC segments followed the protocol of Hofer and Frahm [64] as illustrated in Figure 2A. Segment reconstructions were visually inspected and, if necessary, additional gates were placed to exclude streamlines inconsistent with the known anatomy of the CC.

3.7.2 SMA-putamen pathway

One axial way-point ROI was placed around the putamen and one axial ROI around the supplementary motor cortex [88] (Figure 2B). A way-point gate to exclude fibres projecting to the brain stem was placed inferior to the putamen.

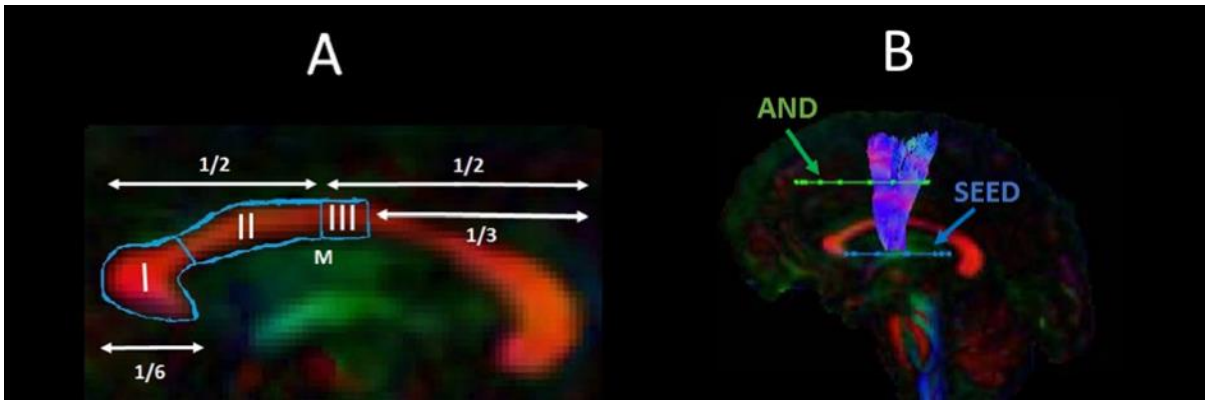

Figure 2.

3.8 Statistical analyses

Statistical analyses were carried out in R Statistical Software (Foundation for Statistical Computing, Vienna, Austria).

3.8.1 Assessment of training effects on drumming performance

Improvements in drumming performance were analysed with a two-way mixed analysis of variance (ANOVA) testing for the effects of group (HD/controls), time of assessment (before/after the training) and group by time interaction effects. We also confirmed detected effects to the ones obtained by running a robust mixed ANOVA, using the bwtrim R function from the WRS2 package [89]. This implements robust methods for statistical estimation and therefore provides a good option to deal with data presenting small sample sizes, skewed distributions and outliers [90]. Significant effects were further explored with post-hoc paired and independent t-tests. The reliability of the post-hoc analyses was assessed with bootstrap analysis based on 1000 samples and the 95% confidence interval (CI) of the mean difference is provided for each significant comparison.

3.8.2 Assessment of group differences in the effect of training on cognitive performance

Performance measures in executive function tasks have been shown to share underlying cognitive structures [91]. Therefore, PCA was employed to reduce the complexity of the cognitive data and hence the problem of multiple comparisons as well as to increase experimental power. PCA was run on change scores for all participants across both groups. Due to the relatively small sample size, we first confirmed with the Kaiser-Meyer-Olkin (KMO) test that our data was suited for PCA. Subsequently, we followed guidelines to limit the number of extracted components [92,93], as follows: first, we employed the Kaiser criterion of including all components

with an eigenvalue greater than 1; second, we inspected the Cattell scree plot [94] to identify the minimal number of components that accounted for most variability in the data; third, we assessed each component's interpretability. A PCA procedure with orthogonal Varimax rotation of the component matrix was used. Loadings that exceeded a value of 0.5 were considered as significant.

Next, we assessed group differences in the component scores with permutation analyses, to understand whether the training had differentially affected HD patients as compared to controls. Permutation testing relies only on minimal assumptions and can therefore be applied when the assumptions of a parametric approach are untenable such as in the case of small sample sizes. Significant group differences were tested using 5,000 permutations and the effect sizes of significant differences were assessed with Cohen's d [95]. Multiple comparison correction was based on a 5% false discovery rate (FDR) using the Benjamini-Hochberg procedure [96].

3.8.3 Training effects on WM microstructure

Median measures of FA, RD, Fr and MPF were derived for each of the reconstructed tracts in ExploreDTI [79]. A percentage change score in these measures between baseline and post-training was calculated in each tract (CCI, CCII, CCIII, left and right SMA-Putamen).

Previous research has shown that variation in the microstructural properties of WM may represent a global effect, rather than being specific to individual tracts, and that WM measures are highly correlated across WM areas [56,97,98]. Therefore, we inspected the inter-tract correlation for each of microstructural metric and found that MPF values were highly correlated, whereas this was not true for the other metrics (Figure 3). Hence, percentage change scores in MPF across the different tracts were transformed with PCA to extract meaningful anatomical properties, following the

362 procedure described above for the PCA of cognitive change scores. PC scores for
363 each participant were then used as dependent variables in a permutation-based
364 analysis using 5,000 permutations to assess group differences in training associated
365 changes in MPF. Finally, as a post-hoc exploration, we looked for between-groups
366 differences in MPF changes in the individual tracts using 5000 permutations.

367 Training-associated changes in FA, Fr and RD were investigated with
368 permutation analyses separately for each tract. Significant group differences in these
369 measures were tested using 5,000 permutations. Multiple comparison correction was
370 based on a 5% FDR using the Benjamini-Hochberg procedure [96]. Cohen's d [95]
371 was used to assess the effect size for those changes found to be significant.

372 3.8.4 Training effects on WM microstructure

373 TBSS [70] was carried out to investigate baseline differences in MPF between
374 HD subjects and healthy controls, , to gain a better insight into differences in training-
375 associated changes. To produce significance maps, a voxel-wise analysis was
376 performed on the MPF projected 4D data for all voxels with FA ≥ 0.20 to exclude
377 peripheral tracts where significant inter-subject variability exists. Inference based on
378 permutations (5,000 permutations) and threshold-free-cluster-enhancement was
379 used. The significance level was set at $p < 0.05$ and corrected by multiple comparisons
380 (family-wise error, FWE).

381 3.8.5 Relationship between changes in MRI measures and changes in drumming and
382 cognitive performance

383 We computed percentage change scores for the drumming performance, in the
384 same way cognitive change scores were calculated. Scores were computed for the
385 easy test pattern in patients and for the medium test pattern in controls, as these
386 training patterns showed a significant improvement in the two groups, respectively.

Spearman correlation coefficients were calculated between drumming and cognitive performance, and microstructural components that showed significant group differences, to assess whether microstructural changes were related to any drumming and/or cognitive benefits of the training.

3.8.6 Exploration of the possible confounding effects of differences in training-compliance and IQ

We examined the training diaries of each participant to assess compliance with training. Each session was marked as completed if the whole 15 minute session had been carried out. Each participant was assigned a score representing the number of training sessions they performed (e.g. a score of 40 if 40 sessions had been carried out). We then assessed group differences with permutation analyses, to test whether there was a significant difference in the amount of training sessions carried out by the groups, and hence understand whether this variable had to be accounted for in the analysis. Significant group differences were tested using 5,000 permutations.

Finally, as there was a significant difference in IQ between patients and controls (Table 2), we investigated whether any training-associated change might be due to differences in premorbid intelligence. The sample size of this experiment was very small, and therefore it was not possible to perform a multiple regression or an analysis of covariance (ANCOVA), to understand the possible influence of IQ as confounding variable. Accordingly, the statistical power to establish the incremental validity of a covariate in explaining an outcome has been shown to be extremely low, and therefore to require large sample sizes [99]. As a potential solution to this issue, we instead performed separate non-parametric Spearman correlation analyses between NART-IQ scores (as this test showed the largest difference between groups), and MRI and cognitive measures showing significant training effects; this allowed us to gain some

412 insight into whether there was a significant association between premorbid intelligence
413 and training-associated changes.
414
415
416 ## *4. Results*
417 ### *4.1 Training effects on drumming performance*
418 The mixed ANOVA of drumming performance for the easy and medium test
419 pattern showed a significant effect of group [easy: $F(1,17) = 22.3$, $p < 0.001$; medium:
420 $F(1,17) = 13.1$, $p = 0.002$] and time [easy: $F(1,17) = 12.83$, $p = 0.004$; medium: $F(1,17)$
421 $= 13.4$, $p = 0.002$] but no interaction (easy: $p = 0.8$; medium: $p = 0.3$). For the hard test
422 pattern there was only a significant effect of group [$F(1,17) = 9.95$, $p = 0.006$] but not
423 of time ($p = 0.1$) and there was no interaction ($p = 0.4$). Results from the robust mixed
424 ANOVA were largely consistent with the above. Specifically, the easy and medium test
425 patterns showed a significant effect of group (easy: $p = 0.002$; medium: $p = 0.02$) and
426 time (easy: $p = 0.04$; medium: $p = 0.049$) but no interaction (easy: $p = 0.45$; medium:
427 $p = 0.69$). The hard test pattern showed a significant effect of group ($p = 0.02$) but not
428 of time ($p = 0.22$) and no interaction ($p = 0.8$). Figure 4 summarises the average
429 drumming performance per group and time point. Overall patients' drumming
430 performance was poorer than controls. Patients improved their drumming
431 performance significantly for the easy pattern [$t(10) = 2.7$, $p = 0.02$; 95% CI of mean
432 difference: 1.5 – 7.8] and controls for the medium pattern [$t(7) = 3.8$, $p = 0.01$; 95% CI
433 of mean difference: 2.8 – 8.5].
434
435 ### *4.2 Group differences in the effect of training on cognitive performance*

Three components, accounting for 79% of the variance in performance improvement in the cognitive benchmark tests, were extracted. The first component loaded highly on performance changes in the dual task (total number of boxes identified under dual task condition), the Stroop task (Stroop interference score), and the trails making task (Trail test switching). Since these variables all measure executive functions including focused attention and distractor suppression, the first component was labelled “executive” component. The second component loaded on variables reflecting the ability to correctly recall digits sequences (i.e. number of correct digits recalled under single and dual task condition) and was therefore labelled “working memory capacity” component. Finally, the third extracted component loaded highly on verbal and category fluency and was therefore labelled “fluency” component (Table 5).

We tested whether the two groups differed in terms of post-training cognition changes, by running permutation analyses on the individual scores for the three extracted components. The two groups differed in the executive component ($t = -1.03$, $p = 0.008$, FDR-corrected $p = 0.024$, $d = 1.15$). However, no significant group differences were detected in the other two components (Working Memory capacity: $t = -0.22$, $p = 0.3296$, FDR-corrected $p = 0.3296$; Fluency: $t = -0.39$, $p = 0.242$ FDR corrected $p = 0.3296$).

4.3 Training effects on WM microstructure

Table 6 reports a summary of the training associated changes in FA, RD, Fr and MPF, across the different tracts.

4.3.1 Training-associated group differences in FA

Permutation analyses of FA changes across the different tracts revealed no significant differences between HD and control groups [CCI: t = 1.22, p = 0.91 (FDR-corrected); CCII: t = 2.65, p = 0.91 (FDR-corrected); CCIII: t = 0.325, p = 0.13 (FDR-corrected); right SMA-Putamen: t = -9.54, p = 0.10 (FDR-corrected); left SMA-Putamen: t = 5.16, p = 0.77 (FDR-corrected).

4.3.2 Training-associated group differences in RD

There were no significant differences in RD changes following training between HD patients and controls [CCI: t = -0.48, p = 0.45 (FDR-corrected); CCII: t = -1.29, p = 0.45 (FDM-corrected); CCIII: t = -1.04, p = 0.45 (FDR-corrected); right SMA-Putamen, t = 4.01 , p = 0.81 (FDR-corrected); left SMA-Putamen, t = -3.68, p = 0.39 (FDR-corrected).

4.3.3 Training-associated group differences in Fr

Permutation analyses of Fr changes across the different tracts revealed no significant differences between HD and control groups [CCI: t = 3.39, p = 0.82 (FDR-corrected; CCII: t = -0.17, p = 0.82 FDR-corrected; CCIII: t = 3.08, p = 0.82 (FDR-corrected); right SMA-Putamen: t = -5.24, p = 0.82 (FDR-corrected); left SMA-Putamen: t = 1.05, p = 0.82 (FDR-corrected)].

4.3.4 Training-associated group differences in MPF

PCA of change scores in MPF revealed one single component explaining 70.2% of the variance. This component presented high loadings from all the tracts investigated. A significant group difference was found for the MPF change-score component, indicating that HD patients presented significantly greater MPF changes in response to training, as compared to controls [t(14) = -1.743, n = 17, p = 0.03, d = 1.796].

Finally, we found a significant difference in mean MPF change scores between the two groups for CCII [t(14) = -20.72, p = 0.04, d = 0.93], CCIII [t(14) = -25.87, p = 0.04, d = 1.07], and the right SMA-putamen pathway [t(14) = -25.48, p = 0.04, d = 1.15] after FDR correction, therefore indicating that there was a differential group effect of training on MPF within these tracts (Figure 5).

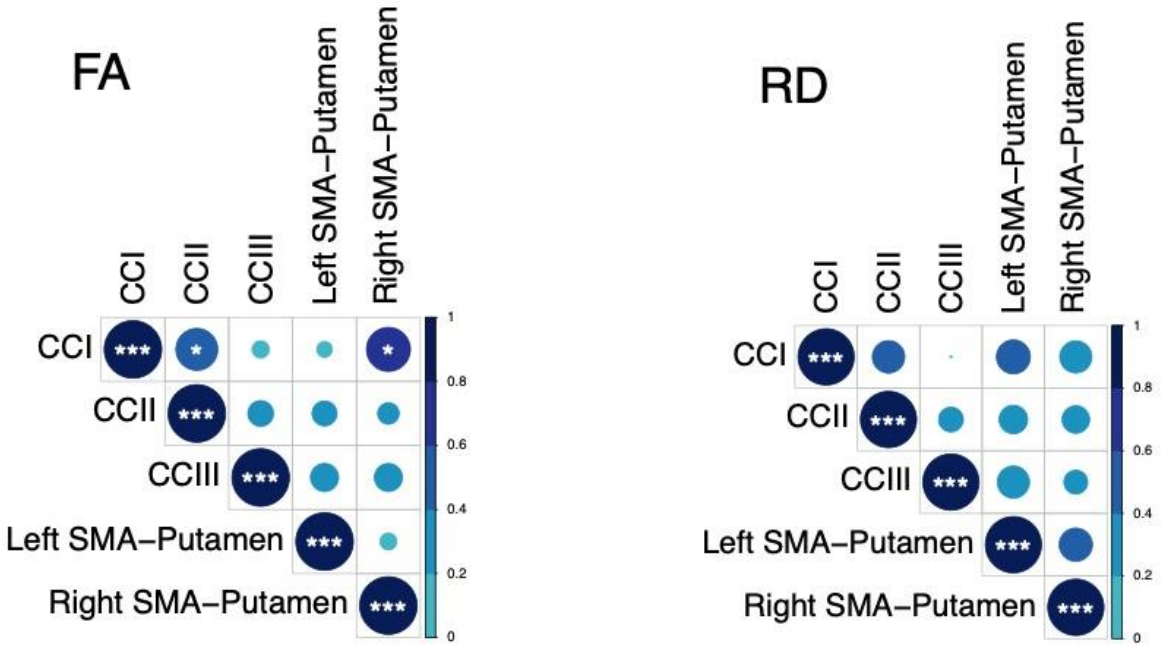

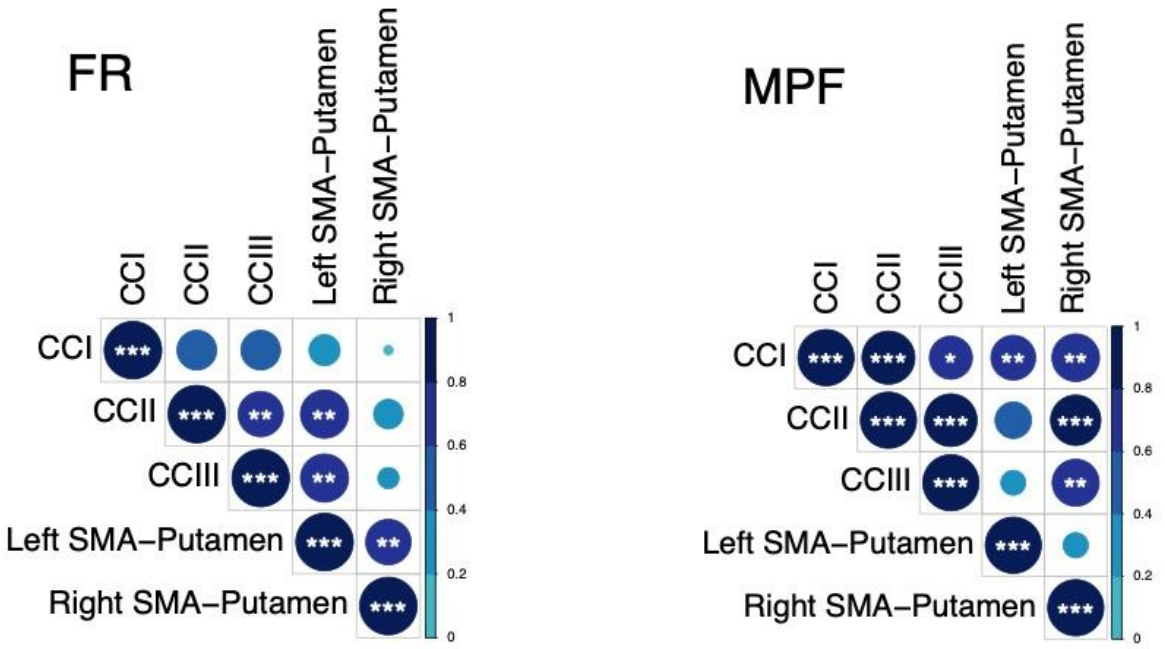

Figure 3.

4.4 Relationship between training-associated changes in MRI measures, and changes in drumming and cognitive performance.

We did not find a significant association between the 'MPF' component scores and improvement in drumming performance (PC1: rho = -0.14, p > 0.05). Moreover, although no significant correlation was observed between the 'Executive' and the 'MPF' component scores, there was a positive trend (rho = .348, p = .171).

4.5 Baseline differences in MPF

Baseline MPF was reduced in the HD group compared to controls, in the midbody of the CC (t = 3.13, p = .05, FWE corrected). Figure 6 shows the areas with reduced MPF in HD patients, in blue.

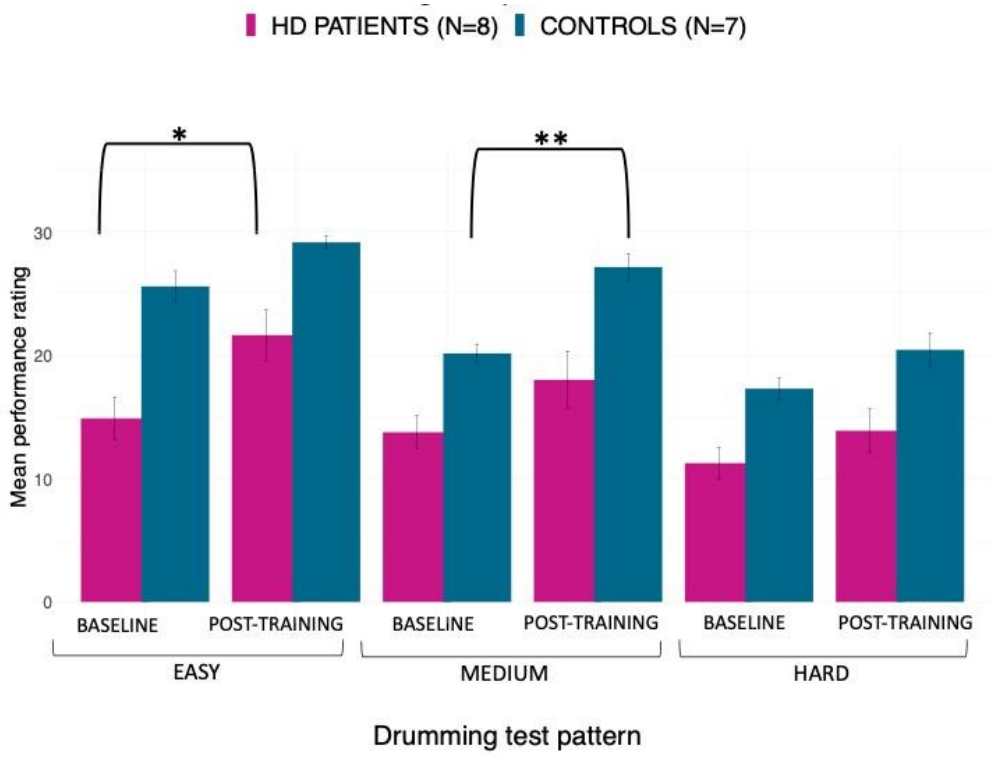

Figure 4.

4.6. Exploration of the possible confounding effects of differences in training-compliance and IQ

The permutation analysis of training compliance revealed that there was not a significant difference in the number of training sessions between HD patients (mean = 38.1, SD = 4.2) and healthy controls (mean = 39.6, SD = 1.2), t = 1.45, p = 0.76. Therefore, the total time spent training should not have influenced any training-associated change in microstructure and/or cognitive measures. Furthermore, we did not detect a significant association of participants' NART-IQ scores with 'MPF' component scores (rho = -0.4, p = 0.10), nor with 'Executive' component scores (rho = -0.34, p = 0.18), suggesting that premorbid intelligence should not have had an influence on training-associated effects.

5. Discussion

Based on evidence that myelin impairment contributes to WM damage in HD [3], and the suggestion that myelin plasticity underlies the learning of new motor skills [27,38], the present study explored whether two months of drumming training would result in changes in WM microstructure in HD patients. Specifically, we expected to detect changes in MPF, as marker of WM myelin plasticity, in HD patients relative to healthy controls.

Firstly, we demonstrated a behavioural effect of the training by showing a significant improvement in drumming performance in patients (easy test pattern) and controls (medium test pattern). We did not detect any group differences in training-associated changes in the diffusion based indices of FA, RD and Fr. However, as hypothesised, we found a group difference in training-induced changes in the MPF PCA component. Specifically, HD patients showed significantly higher increases in MPF relative to controls. Furthermore, through exploratory post-hoc investigations, we detected significantly higher training-induced MPF changes within the CCII, CCIII and the right SMA-putamen pathway between patients and controls. Additionally, TBSS analysis of baseline differences in MPF suggested partial overlap of WM areas showing significant MPF reductions at baseline with areas showing changes post-training (i.e. CCII and CCIII).

MPF can be affected by inflammation [100] and in advanced HD it is likely that inflammation goes hand-in-hand with myelin breakdown [101]. However, a recent CSF biomarker study found no evidence of neuro-inflammation in early-manifest HD [102]. Furthermore, recent evidence shows that this measure may be inconsistent when investigated in relatively small WM areas, presumably because of the effect of spatial heterogeneity in myelin thickness [103]. Nevertheless, the within-subjects design

550 employed in the present study should have helped to minimise noise due to the spatial
551 inconsistency of this measure. Therefore, though preliminary and based on a small
552 sample size, these findings suggest that two months of drumming and rhythm
553 exercises may result in myelin remodelling in patients with early HD.

554 It is plausible that this group difference arose due to WM microstructural
555 differences between patients and controls before the training. Accordingly, the HD
556 group showed a significantly lower baseline MPF, consistent with lower myelin content
557 [3]. Furthermore, previous studies have reported that training-associated percentage
558 changes in MRI measures tend to be higher in patients than in healthy subjects [34].
559 One possibility is that in the healthy brain, neural networks may be optimally
560 myelinated, and further increasing myelin may not improve performance [104–106].
561 Hence, the MPF changes in patients relative to controls might depict mainly a 'catch-
562 up effect' to the better baseline status of the control group. However, disentangling the
563 impact of prior WM microstructural differences on microstructural plasticity during
564 learning is beyond the scope of the current work.

565 Notably, the behavioral effect of drumming training and cognition differed
566 between patients and controls. Patients improved in the easy drumming test pattern,
567 and controls improved in the medium test pattern. Furthermore, consistent with
568 evidence from our pilot study [25], patients showed increases in the executive function
569 components whilst control participants did not show improvements in their cognition.
570 Therefore, inter-group differences in microstructural changes might not only be due to
571 baseline WM microstructural differences, but also to a different behavioral effect of the
572 task between HD subjects and controls. For instance, control participants performed
573 close to ceiling in the easy test pattern, and as the training was tailored to patients'
574 needs, some of the earlier practice sessions may not have optimally challenged them.

The fact that the training seemed more taxing for patients than controls may also explain why improvements in executive functions and changes in MPF were only observed for the patients. Interestingly, baseline IQ was significantly different between the two groups, and this might have had some influence on training performance and on training-associated effects. Here, we failed to find an association between IQ scores and changes in MRI and cognitive measures. However, future studies with larger sample sizes might allow to utilize more advanced statistical approaches, such as an ANCOVA, to better model the possible influence of premorbid IQ on training effects, both at the neural and cognitive level.

A critical question relevant to all training studies concerns the functional significance of any observed neural changes. If, and to what degree adaptive alterations in myelin content can facilitate behavioural change remains poorly understood [105]. In the present study, no significant relationships between changes in MRI measures and changes in drumming proficiency or performance in cognitive tests were found. This might have been due to non-specific training-related neural responses. Specifically, while the training exercise might have triggered changes in brain structure, training-induced changes may not necessarily co-vary with improvements in performance. Alternatively, it might be that the study was insufficiently powered to detect brain-function correlations. The minimum sample size required to detect a correlation was calculated to be 64 people ($\alpha = 0.05$; 80% power; medium effect size; GPower 3 software). Therefore, these results need replication in larger samples. A lack of correlation between structural and functional changes after training has been reported in other studies (including well-powered studies) and may suggest that these processes follow different time courses and/or may occur in different brain regions [107].

It is important to note that our study did not include a non-intervention patient group. Within the 12 month time period of this study it was not possible to recruit a sufficiently large number of well-matched patient controls. Therefore, we cannot disentangle the effects of the training on WM microstructure from HD-associated pathological changes. However, given that HD is a progressive neurodegenerative disease associated with demyelination [3], it is unlikely that increases in MPF observed in the patient group were due to the disease itself. Finally, while the majority of training studies assess brain structural changes between baseline and post-training [34], presumably on account of cost and participant compliance, we suggest that acquiring intermittent scans during the training period could have helped to better capture and understand changes in WM microstructure observed in this study. Accordingly, future studies might be able to provide greater insights into the complex nonlinear relationships between structural changes and behaviour [108].

To conclude, we have demonstrated that two months of drumming and rhythm exercises result in a significantly greater change in a proxy MRI measure of myelin in patients with HD relative to healthy controls. Whilst the current results require replication in a larger patient group with an appropriately matched patient control group, they suggest that behavioural stimulation may result in neural benefits in HD that could be exploited for future therapeutics aiming to delay disease progression.

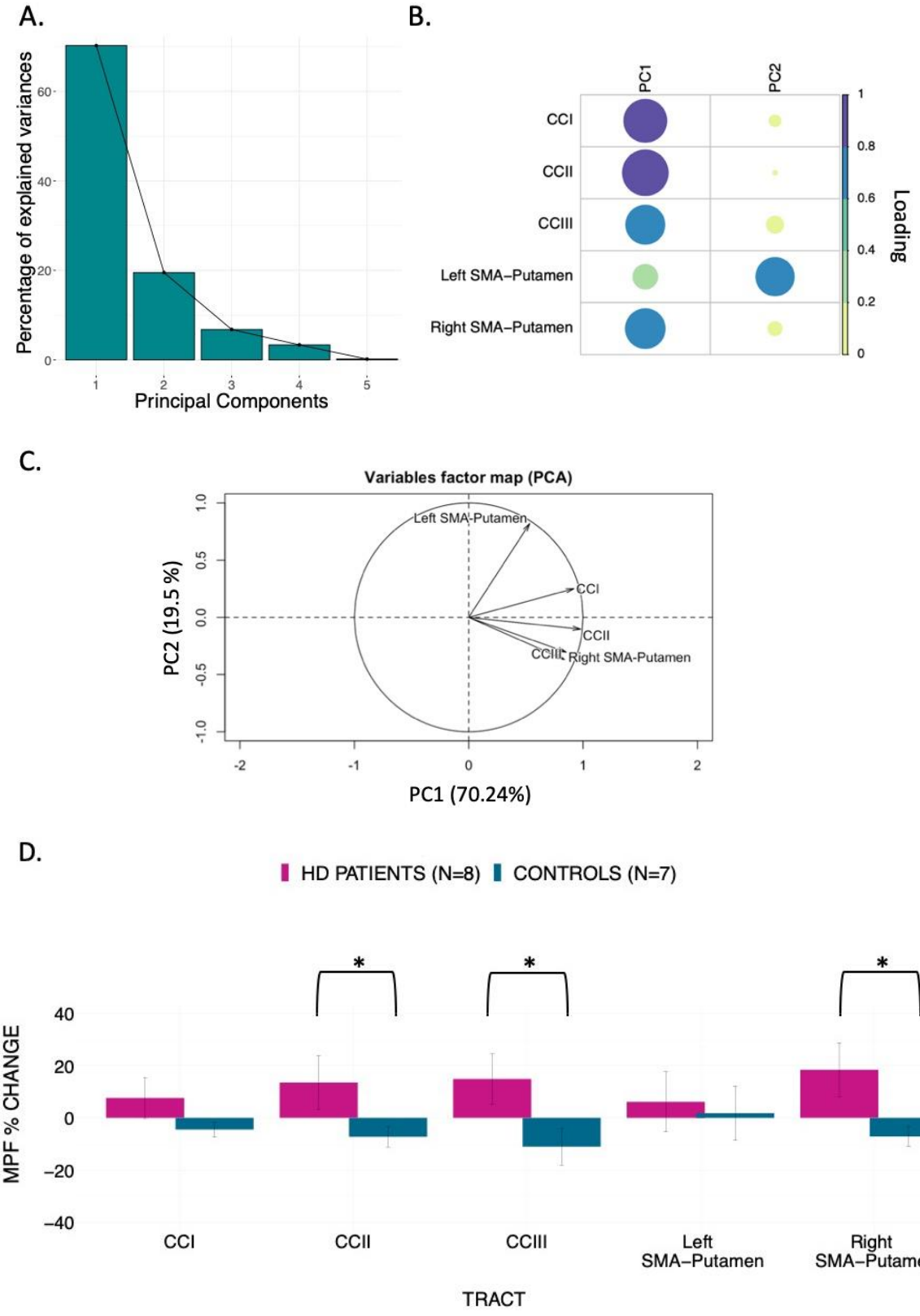
A.
Percentage of explained variances
Principal Components
B.
PC1
PC2
CCI
CCII
CCIII
Left SMA–Putamen
Right SMA–Putamen
Loading
C.
Variables factor map (PCA)
Left SMA-Putamen
CCI
CCII
CCIII
Right SMA-Putamen
PC2 (19.5 %)
PC1 (70.24%)
D.
HD PATIENTS (N=8)
CONTROLS (N=7)
MPF % CHANGE
CCI
CCII
CCIII
Left SMA–Putamen
Right SMA–Putamen
TRACT

Figure 5.

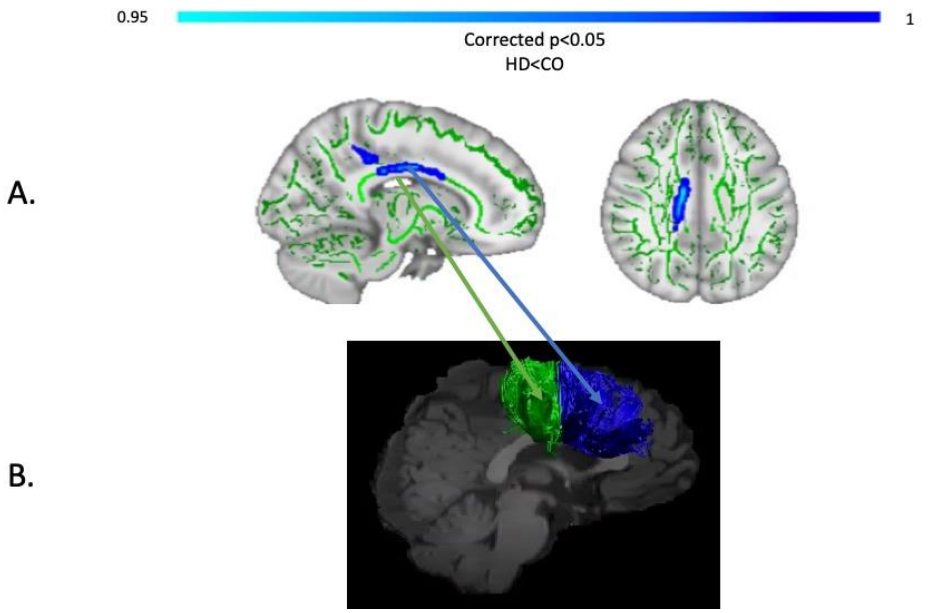

627

628 ***Figure 6.***

629

630

631

632

633

634

635 **Funding & Acknowledgements**

636 The present research was funded by a Wellcome Trust Institutional Strategic Support
637 Fund Award (ref: 506408) to CMB, AR, and DKJ and a Wellcome Trust PhD
638 studentship to CC (ref: 204005/Z/16/Z); DKJ is supported by a New Investigator Award
639 from the Wellcome Trust (ref: 096646/Z/11/Z). We would like to thank Candace
640 Ferman and Louise Gethin for collating the patients' clinical details and Jilu Mole for
641 assistance with data analysis. This manuscript has been released as a pre-print at
642 bioRxiv: https://biorxiv.org/cgi/content/short/2019.12.24.887406v1

643

644

References

[1] Weaver KE, Richards TL, Liang O, Laurino MY, Samii A, Aylward EH. Longitudinal diffusion tensor imaging in Huntington's Disease. Exp Neurol 2009;216:525–9. https://doi.org/10.1016/j.expneurol.2008.12.026.

[2] Bardile CF, Garcia-Miralles M, Caron N, Langley S, Teo RTY, Petretto E, et al. A43 Intrinsic mutant HTT-mediated defects in oligodendroglia cells contribute to myelin deficits and behavioural abnormalities in huntington disease. J Neurol Neurosurg Psychiatry 2018;89:A15–6. https://doi.org/10.1136/jnnp-2018-EHDN.41.

[3] Bartzokis G, Lu PH, Tishler TA, Fong SM, Oluwadara B, Finn JP, et al. Myelin breakdown and iron changes in Huntington's disease: pathogenesis and treatment implications. Neurochem Res 2007;32:1655–64. https://doi.org/10.1007/s11064-007-9352-7.

[4] Beglinger LJ, Langbehn DR, Duff K, Stierman L, Black DW, Nehl C, et al. Probability of obsessive and compulsive symptoms in Huntington's disease. Biol Psychiatry 2007;61:415–8. https://doi.org/10.1016/j.biopsych.2006.04.034.

[5] Ciarmiello A, Cannella M, Lastoria S, Simonelli M, Frati L, Rubinsztein DC, et al. Brain white-matter volume loss and glucose hypometabolism precede the clinical symptoms of Huntington's disease. J Nucl Med Off Publ Soc Nucl Med 2006;47:215–22.

[6] Gregory S, Crawford H, Seunarine K, Leavitt B, Durr A, Roos RAC, et al. Natural biological variation of white matter microstructure is accentuated in Huntington's disease. Hum Brain Mapp 2018;39:3516–27. https://doi.org/10.1002/hbm.24191.

[7] Paulsen JS, Langbehn DR, Stout JC, Aylward E, Ross CA, Nance M, et al. Detection of Huntington's disease decades before diagnosis: the Predict-HD study. J Neurol Neurosurg Psychiatry 2008;79:874–80. https://doi.org/10.1136/jnnp.2007.128728.

669 [8] Rosas HD, Wilkens P, Salat DH, Mercaldo ND, Vangel M, Yendiki AY, et al. Complex
670 spatial and temporally defined myelin and axonal degeneration in Huntington disease.
671 NeuroImage Clin 2018;20:236–42. https://doi.org/10.1016/j.nicl.2018.01.029.
672 [9] Wang N, Yang XW. Huntington Disease's Glial Progenitor Cells Hit the Pause Button in
673 the Mouse Brain. Cell Stem Cell 2019;24:3–4.
674 https://doi.org/10.1016/j.stem.2018.12.004.
675 [10] Gómez-Tortosa E, MacDonald ME, Friend JC, Taylor SA, Weiler LJ, Cupples LA, et al.
676 Quantitative neuropathological changes in presymptomatic Huntington's disease. Ann
677 Neurol 2001;49:29–34.
678 [11] Huang B, Wei W, Wang G, Gaertig MA, Feng Y, Wang W, et al. Mutant huntingtin
679 downregulates myelin regulatory factor-mediated myelin gene expression and affects
680 mature oligodendrocytes. Neuron 2015;85:1212–26.
681 https://doi.org/10.1016/j.neuron.2015.02.026.
682 [12] Jin J, Peng Q, Hou Z, Jiang M, Wang X, Langseth AJ, et al. Early white matter
683 abnormalities, progressive brain pathology and motor deficits in a novel knock-in mouse
684 model of Huntington's disease. Hum Mol Genet 2015;24:2508–27.
685 https://doi.org/10.1093/hmg/ddv016.
686 [13] Myers RH, Vonsattel JP, Paskevich PA, Kiely DK, Stevens TJ, Cupples LA, et al.
687 Decreased Neuronal and Increased Oligodendroglial Densities in Huntington's Disease
688 Caudate Nucleus. J Neuropathol Exp Neurol 1991;50:729–42.
689 https://doi.org/10.1097/00005072-199111000-00005.
690 [14] Simmons DA, Casale M, Alcon B, Pham N, Narayan N, Lynch G. Ferritin accumulation
691 in dystrophic microglia is an early event in the development of Huntington's disease.
692 Glia n.d.;55:1074–84. https://doi.org/10.1002/glia.20526.

693 [15] Teo RTY, Hong X, Yu-Taeger L, Huang Y, Tan LJ, Xie Y, et al. Structural and molecular
694 myelination deficits occur prior to neuronal loss in the YAC128 and BACHD models of
695 Huntington disease. Hum Mol Genet 2016;25:2621–32.
696 https://doi.org/10.1093/hmg/ddw122.
697 [16] Martenson RE. Myelin. CRC Press; 1992.
698 [17] Han I, You Y, Kordower JH, Brady ST, Morfini GA. Differential vulnerability of neurons
699 in Huntington's disease: the role of cell type-specific features. J Neurochem
700 2010;113:1073–91. https://doi.org/10.1111/j.1471-4159.2010.06672.x.
701 [18] Barker R, Mason SL. The hunt for better treatments for Huntington's disease. Lancet
702 Neurol 2019;18:131–3. https://doi.org/10.1016/S1474-4422(18)30448-4.
703 [19] Shannon KM. Recent Advances in the Treatment of Huntington's Disease: Targeting
704 DNA and RNA. CNS Drugs 2020;34:219–28. https://doi.org/10.1007/s40263-019-
705 00695-3.
706 [20] Wood NI, Glynn D, Morton AJ. "Brain training" improves cognitive performance and
707 survival in a transgenic mouse model of Huntington's disease. Neurobiol Dis
708 2011;42:427–37. https://doi.org/10.1016/j.nbd.2011.02.005.
709 [21] Yhnell E, Lelos MJ, Dunnett SB, Brooks SP. Cognitive training modifies disease
710 symptoms in a mouse model of Huntington's disease. Exp Neurol 2016;282:19–26.
711 https://doi.org/10.1016/j.expneurol.2016.05.008.
712 [22] Yhnell E, Furby H, Breen RS, Brookes-Howell LC, Drew CJG, Playle R, et al. Exploring
713 computerised cognitive training as a therapeutic intervention for people with
714 Huntington's disease (CogTrainHD): protocol for a randomised feasibility study. Pilot
715 Feasibility Stud 2018;4:45. https://doi.org/10.1186/s40814-018-0237-0.

716 [23] Caeyenberghs K, Metzler-Baddeley C, Foley S, Jones DK. Dynamics of the Human
717 Structural Connectome Underlying Working Memory Training. J Neurosci Off J Soc
718 Neurosci 2016;36:4056–66. https://doi.org/10.1523/JNEUROSCI.1973-15.2016.
719 [24] Taubert M, Lohmann G, Margulies DS, Villringer A, Ragert P. Long-term effects of
720 motor training on resting-state networks and underlying brain structure. NeuroImage
721 2011;57:1492–8. https://doi.org/10.1016/j.neuroimage.2011.05.078.
722 [25] Metzler-Baddeley C, Cantera J, Coulthard E, Rosser A, Jones DK, Baddeley RJ.
723 Improved Executive Function and Callosal White Matter Microstructure after Rhythm
724 Exercise in Huntington's Disease. J Huntingt Dis 2014;3:273–83.
725 https://doi.org/10.3233/JHD-140113.
726 [26] Drijkoningen D, Caeyenberghs K, Leunissen I, Vander Linden C, Leemans A, Sunaert S,
727 et al. Training-induced improvements in postural control are accompanied by alterations
728 in cerebellar white matter in brain injured patients. NeuroImage Clin 2014;7:240–51.
729 https://doi.org/10.1016/j.nicl.2014.12.006.
730 [27] Scholz J, Klein MC, Behrens TEJ, Johansen-Berg H. Training induces changes in white
731 matter architecture. Nat Neurosci 2009;12:1370–1. https://doi.org/10.1038/nn.2412.
732 [28] Hu Y, Geng F, Tao L, Hu N, Du F, Fu K, et al. Enhanced white matter tracts integrity in
733 children with abacus training. Hum Brain Mapp 2011;32:10–21.
734 https://doi.org/10.1002/hbm.20996.
735 [29] Bengtsson SL, Nagy Z, Skare S, Forsman L, Forssberg H, Ullén F. Extensive piano
736 practicing has regionally specific effects on white matter development. Nat Neurosci
737 2005;8:1148–50. https://doi.org/10.1038/nn1516.
738 [30] Han Y, Yang H, Lv Y-T, Zhu C-Z, He Y, Tang H-H, et al. Gray matter density and white
739 matter integrity in pianists' brain: A combined structural and diffusion tensor MRI study.
740 Neurosci Lett 2009;459:3–6. https://doi.org/10.1016/j.neulet.2008.07.056.

741 [31] Takeuchi H, Sekiguchi A, Taki Y, Yokoyama S, Yomogida Y, Komuro N, et al. Training
742 of working memory impacts structural connectivity. J Neurosci Off J Soc Neurosci
743 2010;30:3297–303. https://doi.org/10.1523/JNEUROSCI.4611-09.2010.
744 [32] Mackey A, Whitaker K, Bunge S. Experience-dependent plasticity in white matter
745 microstructure: reasoning training alters structural connectivity. Front Neuroanat
746 2012;6:32. https://doi.org/10.3389/fnana.2012.00032.
747 [33] Tang Y-Y, Lu Q, Fan M, Yang Y, Posner MI. Mechanisms of white matter changes
748 induced by meditation. Proc Natl Acad Sci 2012;109:10570–4.
749 https://doi.org/10.1073/pnas.1207817109.
750 [34] Caeyenberghs K, Clemente A, Imms P, Egan G, Hocking DR, Leemans A, et al. Evidence
751 for Training-Dependent Structural Neuroplasticity in Brain-Injured Patients: A Critical
752 Review. Neurorehabil Neural Repair 2018;32:99–114.
753 https://doi.org/10.1177/1545968317753076.
754 [35] Gibson EM, Purger D, Mount CW, Goldstein AK, Lin GL, Wood LS, et al. Neuronal
755 Activity Promotes Oligodendrogenesis and Adaptive Myelination in the Mammalian
756 Brain. Science 2014;344:1252304. https://doi.org/10.1126/science.1252304.
757 [36] Mensch S, Baraban M, Almeida R, Czopka T, Ausborn J, El Manira A, et al. Synaptic
758 vesicle release regulates myelin sheath number of individual oligodendrocytes in vivo.
759 Nat Neurosci 2015;18:628–30. https://doi.org/10.1038/nn.3991.
760 [37] Sampaio-Baptista C, Khrapitchev AA, Foxley S, Schlagheck T, Scholz J, Jbabdi S, et al.
761 Motor Skill Learning Induces Changes in White Matter Microstructure and Myelination.
762 J Neurosci 2013;33:19499–503. https://doi.org/10.1523/JNEUROSCI.3048-13.2013.
763 [38] Lakhani B, Borich MR, Jackson JN, Wadden KP, Peters S, Villamayor A, et al. Motor
764 Skill Acquisition Promotes Human Brain Myelin Plasticity. Neural Plast
765 2016;2016:7526135. https://doi.org/10.1155/2016/7526135.

766 [39] Costa RM, Cohen D, Nicolelis MAL. Differential corticostriatal plasticity during fast and
767 slow motor skill learning in mice. Curr Biol CB 2004;14:1124–34.
768 https://doi.org/10.1016/j.cub.2004.06.053.
769 [40] Shmuelof L, Krakauer JW. Are we ready for a natural history of motor learning? Neuron
770 2011;72:469–76. https://doi.org/10.1016/j.neuron.2011.10.017.
771 [41] Steele CJ, Bailey JA, Zatorre RJ, Penhune VB. Early musical training and white-matter
772 plasticity in the corpus callosum: evidence for a sensitive period. J Neurosci Off J Soc
773 Neurosci 2013;33:1282–90. https://doi.org/10.1523/JNEUROSCI.3578-12.2013.
774 [42] Yin HH, Mulcare SP, Hilário MRF, Clouse E, Holloway T, Davis MI, et al. Dynamic
775 reorganization of striatal circuits during the acquisition and consolidation of a skill. Nat
776 Neurosci 2009;12:333–41. https://doi.org/10.1038/nn.2261.
777 [43] Sagi Y, Tavor I, Hofstetter S, Tzur-Moryosef S, Blumenfeld-Katzir T, Assaf Y. Learning
778 in the Fast Lane: New Insights into Neuroplasticity. Neuron 2012;73:1195–203.
779 https://doi.org/10.1016/j.neuron.2012.01.025.
780 [44] Xiao L, Ohayon D, McKenzie IA, Sinclair-Wilson A, Wright JL, Fudge AD, et al. Rapid
781 production of new oligodendrocytes is required in the earliest stages of motor skill
782 learning. Nat Neurosci 2016;19:1210–7. https://doi.org/10.1038/nn.4351.
783 [45] Papoutsi M, Labuschagne I, Tabrizi SJ, Stout JC. The cognitive burden in Huntington's
784 disease: Pathology, phenotype, and mechanisms of compensation. Mov Disord
785 2014;29:673–83. https://doi.org/10.1002/mds.25864.
786 [46] Nakamura T, Nagata M, Yagi T, Graybiel AM, Yamamori T, Kitsukawa T. Learning new
787 sequential stepping patterns requires striatal plasticity during the earliest phase of
788 acquisition. Eur J Neurosci 2017;45:901–11. https://doi.org/10.1111/ejn.13537.

[47] Lanciego JL, Luquin N, Obeso JA. Functional neuroanatomy of the basal ganglia. Cold Spring Harb Perspect Med 2012;2:a009621–a009621. https://doi.org/10.1101/cshperspect.a009621.

[48] Guitar NA, Connelly DM, Nagamatsu LS, Orange JB, Muir-Hunter SW. The effects of physical exercise on executive function in community-dwelling older adults living with Alzheimer's-type dementia: A systematic review. Ageing Res Rev 2018;47:159–67. https://doi.org/10.1016/j.arr.2018.07.009.

[49] Duchesne C, Lungu O, Nadeau A, Robillard ME, Boré A, Bobeuf F, et al. Enhancing both motor and cognitive functioning in Parkinson's disease: Aerobic exercise as a rehabilitative intervention. Brain Cogn 2015;99:68–77. https://doi.org/10.1016/j.bandc.2015.07.005.

[50] Giacosa C, Karpati FJ, Foster NEV, Penhune VB, Hyde KL. Dance and music training have different effects on white matter diffusivity in sensorimotor pathways. NeuroImage 2016;135:273–86. https://doi.org/10.1016/j.neuroimage.2016.04.048.

[51] Pierpaoli C, Basser PJ. Toward a quantitative assessment of diffusion anisotropy. Magn Reson Med 1996;36:893–906.

[52] De Santis S, Drakesmith M, Bells S, Assaf Y, Jones DK. Why diffusion tensor MRI does well only some of the time: Variance and covariance of white matter tissue microstructure attributes in the living human brain. Neuroimage 2014;89:35–44. https://doi.org/10.1016/j.neuroimage.2013.12.003.

[53] Wheeler-Kingshott CAM, Cercignani M. About "axial" and "radial" diffusivities. Magn Reson Med 2009;61:1255–60. https://doi.org/10.1002/mrm.21965.

[54] Sled JG. Modelling and interpretation of magnetization transfer imaging in the brain. NeuroImage 2018;182:128–35. https://doi.org/10.1016/j.neuroimage.2017.11.065.

[55] Assaf Y, Basser PJ. Composite hindered and restricted model of diffusion (CHARMED) MR imaging of the human brain. NeuroImage 2005;27:48–58. https://doi.org/10.1016/j.neuroimage.2005.03.042.

[56] Lövdén M, Bodammer NC, Kühn S, Kaufmann J, Schütze H, Tempelmann C, et al. Experience-dependent plasticity of white-matter microstructure extends into old age. Neuropsychologia 2010;48:3878–83. https://doi.org/10.1016/j.neuropsychologia.2010.08.026.

[57] Zatorre RJ, Fields RD, Johansen-Berg H. Plasticity in gray and white: neuroimaging changes in brain structure during learning. Nat Neurosci 2012;15:528–36. https://doi.org/10.1038/nn.3045.

[58] Serres S, Anthony DC, Jiang Y, Campbell SJ, Broom KA, Khrapitchev A, et al. Comparison of MRI signatures in pattern I and II multiple sclerosis models. NMR Biomed 2009;22:1014–24. https://doi.org/10.1002/nbm.1404.

[59] Ou X, Sun S-W, Liang H-F, Song S-K, Gochberg DF. The MT pool size ratio and the DTI radial diffusivity may reflect the myelination in shiverer and control mice. NMR Biomed 2009;22:480–7. https://doi.org/10.1002/nbm.1358.

[60] Levesque IR, Giacomini PS, Narayanan S, Ribeiro LT, Sled JG, Arnold DL, et al. Quantitative magnetization transfer and myelin water imaging of the evolution of acute multiple sclerosis lesions. Magn Reson Med 2010;63:633–40. https://doi.org/10.1002/mrm.22244.

[61] Schmierer K, Tozer DJ, Scaravilli F, Altmann DR, Barker GJ, Tofts PS, et al. Quantitative Magnetization Transfer Imaging in Postmortem Multiple Sclerosis Brain. J Magn Reson Imaging JMRI 2007;26:41–51. https://doi.org/10.1002/jmri.20984.

836 [62] Barazany D, Basser PJ, Assaf Y. In vivo measurement of axon diameter distribution in
837 the corpus callosum of rat brain. Brain 2009;132:1210–20.
838 https://doi.org/10.1093/brain/awp042.
839 [63] Poudel GR, Stout JC, Domínguez D JF, Salmon L, Churchyard A, Chua P, et al. White
840 matter connectivity reflects clinical and cognitive status in Huntington's disease.
841 Neurobiol Dis 2014;65:180–7. https://doi.org/10.1016/j.nbd.2014.01.013.
842 [64] Hofer S, Frahm J. Topography of the human corpus callosum revisited--comprehensive
843 fiber tractography using diffusion tensor magnetic resonance imaging. NeuroImage
844 2006;32:989–94. https://doi.org/10.1016/j.neuroimage.2006.05.044.
845 [65] Vonsattel JPG, Difiglia M. Huntington Disease. J Neuropathol Exp Neurol 1998;57:369–
846 84. https://doi.org/10.1097/00005072-199805000-00001.
847 [66] Diana Rosas H, Lee SY, Bender A, Zaleta AK, Vange M, Yu P, et al. Altered White
848 Matter Microstructure in the Corpus Callosum in Huntington's Disease: implications for
849 cortical "disconnection." NeuroImage 2010;49:2995–3004.
850 https://doi.org/10.1016/j.neuroimage.2009.10.015.
851 [67] Phillips O, Sanchez-Castaneda C, Elifani F, Maglione V, Pardo AD, Caltagirone C, et al.
852 Tractography of the Corpus Callosum in Huntington's Disease. PLOS ONE
853 2013;8:e73280. https://doi.org/10.1371/journal.pone.0073280.
854 [68] Dumas EM, van den Bogaard SJA, Ruber ME, Reilman RR, Stout JC, Craufurd D, et al.
855 Early changes in white matter pathways of the sensorimotor cortex in premanifest
856 Huntington's disease. Hum Brain Mapp 2012;33:203–12.
857 https://doi.org/10.1002/hbm.21205.
858 [69] Bourbon-Teles J, Bells S, Jones DK, Coulthard E, Rosser A, Metzler-Baddeley C. Myelin
859 Breakdown in Human Huntington's Disease: Multi-Modal Evidence from Diffusion

MRI and Quantitative Magnetization Transfer. Non-Invasive MRI Window Brain Inflamm 2019;403:79–92. https://doi.org/10.1016/j.neuroscience.2017.05.042.

[70] Smith SM, Jenkinson M, Johansen-Berg H, Rueckert D, Nichols TE, Mackay CE, et al. Tract-based spatial statistics: Voxelwise analysis of multi-subject diffusion data. NeuroImage 2006;31:1487–505. https://doi.org/10.1016/j.neuroimage.2006.02.024.

[71] Nasreddine ZS, Phillips NA, Bédirian V, Charbonneau S, Whitehead V, Collin I, et al. The Montreal Cognitive Assessment, MoCA: A Brief Screening Tool For Mild Cognitive Impairment. J Am Geriatr Soc 2005;53:695–9. https://doi.org/10.1111/j.1532-5415.2005.53221.x.

[72] Nelson H. National Adult Reading Test (NART) test manual (Part 1 n.d.

[73] Baddeley A. Exploring the central executive. Q J Exp Psychol A 1996;49A:5–28. https://doi.org/10.1080/027249896392784.

[74] Baldo JV, Shimamura AP, Delis DC, Kramer J, Kaplan E. Verbal and design fluency in patients with frontal lobe lesions. J Int Neuropsychol Soc 2001;7:586–96. https://doi.org/10.1017/S1355617701755063.

[75] Jones DK, Horsfield MA, Simmons A. Optimal strategies for measuring diffusion in anisotropic systems by magnetic resonance imaging. Magn Reson Med 1999;42:515–25.

[76] Cercignani M, Alexander DC. Optimal acquisition schemes for in vivo quantitative magnetization transfer MRI. Magn Reson Med 2006;56:803–10. https://doi.org/10.1002/mrm.21003.

[77] Irfanoglu MO, Walker L, Sarlls J, Marenco S, Pierpaoli C. Effects of image distortions originating from susceptibility variations and concomitant fields on diffusion MRI tractography results. NeuroImage 2012;61:275–88. https://doi.org/10.1016/j.neuroimage.2012.02.054.

885 [78] Leemans A, Jones DK. The B-matrix must be rotated when correcting for subject motion
886 in DTI data. Magn Reson Med 2009;61:1336–49. https://doi.org/10.1002/mrm.21890.
887 [79] Leemans A, Jeurissen B, Sijbers J, Jones D. ExploreDTI: a graphical toolbox for
888 processing, analyzing, and visualizing diffusion MR data. Proc Intl Soc Mag Reson Med,
889 vol. 17, 2009.
890 [80] Pasternak O, Sochen N, Gur Y, Intrator N, Assaf Y. Free water elimination and mapping
891 from diffusion MRI. Magn Reson Med 2009;62:717–30.
892 https://doi.org/10.1002/mrm.22055.
893 [81] Ben-Amitay S, Jones DK, Assaf Y. Motion correction and registration of high b-value
894 diffusion weighted images. Magn Reson Med 2012;67:1694–702.
895 https://doi.org/10.1002/mrm.23186.
896 [82] Klein S, Staring M, Murphy K, Viergever MA, Pluim JPW. elastix: a toolbox for
897 intensity-based medical image registration. IEEE Trans Med Imaging 2010;29:196–205.
898 https://doi.org/10.1109/TMI.2009.2035616.
899 [83] Henkelman RM, Huang X, Xiang QS, Stanisz GJ, Swanson SD, Bronskill MJ.
900 Quantitative interpretation of magnetization transfer. Magn Reson Med 1993;29:759–
901 66.
902 [84] Ramani A, Dalton C, Miller DH, Tofts PS, Barker GJ. Precise estimate of fundamental
903 in-vivo MT parameters in human brain in clinically feasible times. Magn Reson Imaging
904 2002;20:721–31. https://doi.org/10.1016/S0730-725X(02)00598-2.
905 [85] Dell'acqua F, Scifo P, Rizzo G, Catani M, Simmons A, Scotti G, et al. A modified damped
906 Richardson-Lucy algorithm to reduce isotropic background effects in spherical
907 deconvolution. NeuroImage 2010;49:1446–58.
908 https://doi.org/10.1016/j.neuroimage.2009.09.033.

[86] Jeurissen B, Leemans A, Jones DK, Tournier J-D, Sijbers J. Probabilistic fiber tracking using the residual bootstrap with constrained spherical deconvolution. Hum Brain Mapp 2011;32:461–79. https://doi.org/10.1002/hbm.21032.

[87] Catani M, Howard RJ, Pajevic S, Jones DK. Virtual in vivo interactive dissection of white matter fasciculi in the human brain. NeuroImage 2002;17:77–94. https://doi.org/10.1006/nimg.2002.1136.

[88] Leh SE, Ptito A, Chakravarty MM, Strafella AP. Fronto-striatal connections in the human brain: a probabilistic diffusion tractography study. Neurosci Lett 2007;419:113–8. https://doi.org/10.1016/j.neulet.2007.04.049.

[89] Mair P, Wilcox R. Robust statistical methods in R using the WRS2 package. Behav Res Methods 2020;52:464–88. https://doi.org/10.3758/s13428-019-01246-w.

[90] Wilcox RR. Introduction to robust estimation and hypothesis testing. Academic press; 2011.

[91] Testa R, Bennett P, Ponsford J. Factor analysis of nineteen executive function tests in a healthy adult population. Arch Clin Neuropsychol Off J Natl Acad Neuropsychol 2012;27:213–24. https://doi.org/10.1093/arclin/acr112.

[92] Preacher KJ, MacCallum RC. Exploratory Factor Analysis in Behavior Genetics Research: Factor Recovery with Small Sample Sizes. Behav Genet 2002;32:153–61. https://doi.org/10.1023/A:1015210025234.

[93] Winter* JCF de, Dodou* D, Wieringa PA. Exploratory Factor Analysis With Small Sample Sizes. Multivar Behav Res 2009;44:147–81. https://doi.org/10.1080/00273170902794206.

[94] Cattell RB. The Scree Test For The Number Of Factors. Multivar Behav Res 1966;1:245–76. https://doi.org/10.1207/s15327906mbr0102_10.

[95] Cohen J. Statistical power analysis for the behavioral sciences. Academic press; 2013.

[96] Benjamini Y, Hochberg Y. Controlling the False Discovery Rate: A Practical and Powerful Approach to Multiple Testing. J R Stat Soc Ser B Methodol 1995;57:289–300.

[97] Penke L, Maniega SM, Murray C, Gow AJ, Hernández MCV, Clayden JD, et al. A General Factor of Brain White Matter Integrity Predicts Information Processing Speed in Healthy Older People. J Neurosci 2010;30:7569–74. https://doi.org/10.1523/JNEUROSCI.1553-10.2010.

[98] Wahl M, Li Y-O, Ng J, Lahue SC, Cooper SR, Sherr EH, et al. Microstructural correlations of white matter tracts in the human brain. NeuroImage 2010;51:531–41. https://doi.org/10.1016/j.neuroimage.2010.02.072.

[99] Westfall J, Yarkoni T. Statistically Controlling for Confounding Constructs Is Harder than You Think. PLOS ONE 2016;11:e0152719. https://doi.org/10.1371/journal.pone.0152719.

[100] Henkelman RM, Stanisz GJ, Graham SJ. Magnetization transfer in MRI: a review. NMR Biomed n.d.;14:57–64. https://doi.org/10.1002/nbm.683.

[101] Rocha NP, Ribeiro FM, Furr-Stimming E, Teixeira AL. Neuroimmunology of Huntington's disease: revisiting evidence from human studies. Mediators Inflamm 2016;2016.

[102] Vinther-Jensen T, Simonsen AH, Budtz-Jørgensen E, Hjermind LE, Nielsen JE. Ubiquitin: a potential cerebrospinal fluid progression marker in Huntington's disease. Eur J Neurol n.d.;22:1378–84. https://doi.org/10.1111/ene.12750.

[103] Wang Y, van Gelderen P, de Zwart JA, Duyn JH. B0-field dependence of MRI T1 relaxation in human brain. NeuroImage 2020;213:116700. https://doi.org/10.1016/j.neuroimage.2020.116700.

[104] Chomiak T, Hu B. What Is the Optimal Value of the g-Ratio for Myelinated Fibers in the Rat CNS? A Theoretical Approach. PLOS ONE 2009;4:e7754. https://doi.org/10.1371/journal.pone.0007754.

[105] Kaller MS, Lazari A, Blanco-Duque C, Sampaio-Baptista C, Johansen-Berg H. Myelin plasticity and behaviour—connecting the dots. Curr Opin Neurobiol 2017;47:86–92. https://doi.org/10.1016/j.conb.2017.09.014.

[106] Rushton WAH. A theory of the effects of fibre size in medullated nerve. J Physiol 1951;115:101–22.

[107] Valkanova V, Eguia Rodriguez R, Ebmeier KP. Mind over matter--what do we know about neuroplasticity in adults? Int Psychogeriatr 2014;26:891–909. https://doi.org/10.1017/S1041610213002482.

[108] Thomas C, Baker CI. Teaching an adult brain new tricks: A critical review of evidence for training-dependent structural plasticity in humans. NeuroImage 2013;73:225–36. https://doi.org/10.1016/j.neuroimage.2012.03.069.

[109] Trenerry MR, Crosson B, DeBoe J, Leber WR. Stroop neuropsychological screening test. Odessa FL Psychol Assess Resour 1989.

[110] Delis DC, Kramer JH, Kaplan E, Holdnack J. Reliability and validity of the Delis-Kaplan Executive Function System: an update. J Int Neuropsychol Soc JINS 2004;10:301–3. https://doi.org/10.1017/S1355617704102191.

	Age	Length of CAG repeats	TMS	FAS
Mean (Range)	48.5 (22-68)	43.6 (40-51)	18.7 (0-69)	22.6 (17-25)
SD	15.6	3.5	24.7	3.3

Table 1. *Demographics and background clinical information of the patients' cohort. Based on TMS and FAS, most of the patients were at early disease stages, however two of them were more advanced. Abbreviations: CAG = cytosine-adenine-guanine; TMS = Total Motor Score out of 124 (the higher the scores the more impaired the performance); FAS = Functional Assessment Score out of 25 (the higher the scores the better the performance); SD = Standard Deviation.*

Mean (SD, range)	Patients (n = 8)	Controls (n = 9)	Mann-Whitney U (p-value)
Age	48.5 (15.62, 22-68)	52.6 (14.56, 22-68)	U = 31 (p = 0.673)
NART-IQ	106.3 (13.13, 94-123)	121.22 (4.32, 117-128)	U = 8 (p = 0.006)
MoCa	23 (5.6, 14-29)	27.67 (1, 26-29)	U = 14 (p = 0.036)

Table 2. *Demographics and general cognitive profile of patients and controls. Both groups were matched for age, sex and years of education but the patient group had a*

990 *lower NART-IQ and performed less well than the control group in the MoCA.*
991 *Abbreviations: NART-IQ = verbal IQ estimate based on the National Adult Reading*
992 *Test; MoCA = Montreal Cognitive Assessment score out of 30.*
993
994

Task	Outcome variables	Description
Simultaneous box crossing and digit sequences repetition [73]	Correct digits recalled under single task condition; correct digits recalled under dual task conditions; boxes identified under dual task condition.	Correct number of recalled digits in a standard digit span test; correct number of recalled digits in the dual condition; number of boxes identified in the dual condition
Stroop test [109]	Stroop interference score	Calculated by subtracting the number of errors from the total number of items presented in the test
Trials test [73]	Trail test switching	Performance accuracy: reflects the ability of moving flexibly from one set of rules to another in response to changing task requirements

Verbal and category fluency test [110]	Verbal and category fluency	Number of generated words starting with the following letters: “F”, “A”, “S” and “M”, “C”, “R”; number of generated words belonging to the following categories: “animals” and “boys’ names” and “supermarket items” and “girls’ names”

Table 3. *Cognitive outcome variables assessed in this study. Tests were carried out before and after the training, and a percentage change score was computed for each variable.*

	T_1-w	**DTI**	**CHARMED**	**T1 map**	**MT-w**	**B0 map**
Pulse sequence	FSPGR	SE\EPI	SE\EPI	SPGR (3D)	FSPGR (3D)	SPGR (3D)
Matrix size	256×256	96×96	96×96	96×96×60	96×96×60	128×128
FoV (mm)	230	230	230	240	240	220
Slices	172	60	60	-	-	-

Slice thickness (mm)	1	2.4	2.4	-	-	-
TE,TR (ms)	7.8, 2.9	87, 16000	126, 17000	6.85, 1.2	2.18,25.82	TE: 9 & 7 TR: 20
Off-resonance pulses (Hz/°)	-	-	-	-	100[38]0/332, 1000/333, 12062/628, 47185/628, 56363/332, 2751/628, 1000/628, 1000/628, 2768/628, 2791/628, 2887/628	-
Flip angles (°)	20	90	90	15,7,3	5	90

Table 4. *Scan parameters. All sequences were acquired at 3T. For each of the sequences, the main acquisition parameters are provided. T_1-w: T_1-weighted; MT-w: MT-weighted; FSPGR: fast spoiled gradient echo; SE: spin-echo; EPI: echo-planar imaging; SPGR: spoiled gradient recalled-echo; FoV: field of view; TE: echo time; TR: repetition time.*

% Change	Executive	Working memory capacity	Fluency
Total box (dual)	**0.864**	0.022	0.419
Stroop interference score	**0.811**	-0.270	-0.267
Trail test switching	**0.731**	-0.470	0.162
Correct digits under single task condition	0.201	**0.904**	0.129
Correct digits under dual task condition	-0.193	**0.855**	-0.018
Category fluency	-0.070	-0.138	**0.817**
Verbal fluency	-0.026	-0.232	**-0.799**

Table 5. *Rotated Component Loadings on Change in the Cognitive Benchmark Tests. Significant loadings (>0.5) are highlighted in bold.*

FA	t	p	FDR corrected p
CCI	1.220	0.909	0.91
CCII	2.650	0.91	0.91

CCIII	0.320	0.48	0.91
Left SMA-Putamen	5.160	0.77	0.91
Right SMA-Putamen	-9.54	0.02	0.11
RD			
CCI	-0.48	0.35	0.45
CCII	-1.29	0.22	0.45
CCIII	-1.04	0.30	0.45
Left SMA-Putamen	-3.68	0.08	0.39
Right SMA-Putamen	4.010	0.80	0.80
Fr			
CCI	0.033	0.81	0.82
CCII	-0.001	0.49	0.82
CCIII	0.03	0.82	0.82
Left SMA-Putamen	0.01	0.58	0.82
Right SMA-Putamen	-0.052	0.1996	0.817
MPF			
CCI	-12.06	0.08	0.10
CCII	-20.72	0.03	**0.05**

CCIII	-25.87	0.02	**0.05**
Left SMA-Putamen	-4.34	0.38	0.38
Right SMA-Putamen	-25.48	0.02	**0.05**

Table 6. *Summary statistics for the permutation analysis of training effects on FA, RD, Fr and MPF, across the investigated tracts.*

Figure 1. (1) ***pathway regions of interest.*** *Sagittal views of the reconstructed WM pathways displayed on a T_1-weighted image for one control participant. (A) CCI, CCII, and CCIII (Hofer and Frahm, 2006): CCI is the most anterior portion of the CC and maintains prefrontal connections between both hemispheres; CCII is the portion that maintains connections between premotor and supplementary motor areas of both hemispheres. CCIII maintains connections between primary motor cortices of both hemispheres. (B) SMA-putamen pathway: this pathway has efferent and afferent projections to the primary motor cortex and is involved in movement execution.*

Figure 2. Sagittal views of the tractography protocols. *(A) CCI, CCII and CCIII (B) SMA - putamen pathway. Booleian logic OR waypoint regions of interest gates are illustrated in blue; AND gates in green. M = Midline.*

Figure 3. *Correlation matrices for the MRI metrics investigated across the different WM pathways. Colour intensity and the size of the circles are proportional to the*

*strength of the correlation. * p < 0.05, ** p < 0.01, *** p < 0.001. The absolute correlation coefficient is plotted. MPF values were highly correlated across tracts, whereas this was not true for the other metrics*

Figure 4. Mean ratings for drumming performance *according to the Trinity College London marking criteria for percussion (2016) as a function of group and time point. Patients improved their drumming performance significantly for the easy test pattern and controls for the medium difficult test pattern. * p < 0.05, ** p < 0.01, bootstrapping based on 1000 samples.*

Figure 5. MPF changes scores*: PCA scree plot (A); plot summarising how each variable is accounted for in every principal component - colour intensity and the size of the circles are proportional to the loading: PC1 loads on CCI, CCII, CCIII and right SMA-Putamen, while PC2 loads mostly on the left SMA-Putamen; the absolute correlation coefficient is plotted (B); correlation circle, interpreted as follows: 1) positively correlated variables are grouped together, 2) negatively correlated variables are positioned on opposite sides of the plot origin (opposite quadrants), 3) the distance between variables and the origin measures the quality of the variable on the factor map. Variables that are away from the origin are well represented on the factor map (C); Bar graph of the percentage change in MPF across the inspected tracts; Error bars represent the standard error; training was associated with a significantly greater change in MPF in CCII, CCIII, and right SMA-Putamen; * (p<0.05), results corrected for multiple comparisons with FDR (D).*

***Figure 6. TBSS analysis of baseline MPF values (A)**. Light blue areas show a significant reduction of MPF in patients with HD compared to controls ($p < 0.05$, FWE corrected). The midbody of the CC was mostly found to be affected, which carries connections to the premotor, supplementary motor and motor areas of the brain. **Tracts showing significantly greater MPF changes in HD patients post-training as compared to controls (B).** Areas showing significant MPF reductions at baseline overlap with tracts showing significant changes post-training (i.e. CCII and CCIII).*